Yields, Angular Distributions, and Polarization of Gamma Rays from Coulomb Excitation

F. K. McGowan and P. H. Stelson
Oak Ridge National Laboratory, Oak Ridge, Tennessee
(Received October 7, 1957)

The yields of gamma rays resulting from Coulomb excitation have been measured for Tl^{205}, Tl^{203}, Au^{197}, Ir^{193}, Ir^{191}, Re^{187}, Re^{185}, W^{183}, Ta^{181}, Cd^{113}, Cd^{111}, Ag^{109}, Ag^{107}, Rh^{103}, Mo^{95}, Os^{192}, Os^{190}, Os^{188}, W^{186}, W^{184}, and W^{182}. Angular distributions of the gamma radiation from the nuclei Tl^{205}, Tl^{203}, Au^{197}, Ir^{193}, Ir^{191}, Re^{187}, Re^{185}, Ta^{181}, Cd^{113}, Cd^{111}, Ag^{109}, Ag^{107}, Rh^{103}, and Mo^{95} have been measured with respect to the incident proton beam on thick targets. The linear polarization of gamma rays following Coulomb excitation has been studied. A polarimeter based on the Compton scattering mechanism has been constructed and its effectiveness determined by measurements of the known polarization of gamma rays from excitation of 2+ levels in even-even nuclei. Polarization-direction measurements of several transitions in odd-mass nuclei have resolved the ambiguity either in the value of $(E2/M1)^{\frac{1}{2}}$ or in the spin of the excited state deduced from the angular distributions. Reduced transition probabilities for $E2$ and $M1$ transitions are obtained. In some instances these quantities are compared to the predictions of the collective model of the nucleus.

I. INTRODUCTION

PREVIOUSLY we have reported experiments[1] undertaken to test the calculations[2] of the particle parameters a_ν which enter into the expression for the angular distribution of gamma rays following Coulomb excitation. Within the accuracy of the experiments (± 2 to 5% for the particle parameter a_2) there is agreement with the numerical results obtained from the quantum mechanical treatment of the process.

For odd-mass nuclei an angular distribution measurement gives information on the spins of the excited states produced by Coulomb excitation. That is, one measures $A_\nu a_\nu$ and uses the known particle parameters to determine the A_ν which depend on the spins of the levels and the multipole order of the radiation. For mixed $M1$-$E2$ transitions, such as are generally observed in odd-mass nuclei, a measurement of the directional angular correlation affords a sensitive means of determining the ratio $(E2/M1)^{\frac{1}{2}}$ in addition to inferring the spins of the excited states. This information combined with the cross section for excitation yields the reduced transition probability for the magnetic dipole transition. However, several cases have been encountered in which the angular distribution was equally well fitted by two rather different values for $(E2/M1)^{\frac{1}{2}}$. Such an example is shown in Fig. 1 where A_2 is plotted as a function of $\delta=(E2/M1)^{\frac{1}{2}}$ for the spin sequence $\frac{1}{2}(Q)\frac{3}{2}(Q+D)\frac{1}{2}$.

Biedenharn and Rose[3] have expressed in a convenient form the polarization-direction correlation with polarization of the mixed radiation being measured. The correlation function has for a γ-γ cascade the form

$$W(\theta,\phi)=W_{\mathrm{I}}+\delta^2 W_{\mathrm{II}}+2\delta W_{\mathrm{III}},$$

where δ is $(E2/M1)^{\frac{1}{2}}$. W_{I}, W_{II}, and W_{III} are the polarization-direction correlation functions for pure 2^{L_1} pole-pure 2^{L_2} pole, pure 2^{L_1} pole-pure 2^{L_2+1} pole, and the interference term, respectively. ϕ is the angle between the direction of polarization and the normal to the plane defined by the directions of propagation of the two gamma rays in cascade. Calculations of the polarization-direction correlation with polarization of the mixed radiation being measured showed that this correlation was quite different for the two values of $(E2/M1)^{\frac{1}{2}}$. These results are also shown in Fig. 1 for the spin sequence $\frac{1}{2}(Q)\frac{3}{2}(E2+M1)\frac{1}{2}$. The ratio P of the polarization intensities is $W(90°,\phi=90°)/W(90°,\phi=0)$ in the notation of Biedenharn and Rose. For gamma rays following Coulomb excitation, one replaces A_ν appearing in the correlation functions above by $A_\nu a_\nu$, where a_ν is the particle parameter that enters in the Coulomb excitation process, and one takes $L_1=2$ (electric quadrupole excitation).

A polarimeter based on the Compton scattering mechanism has been constructed and its effectiveness

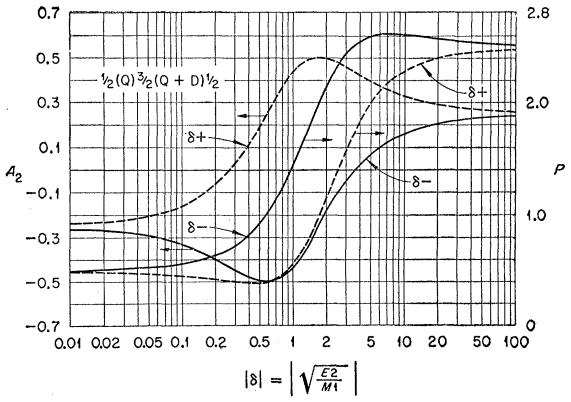

FIG. 1. The ordinate on the left is the angular distribution coefficient A_2 as a function of $\delta=(E2/M1)^{\frac{1}{2}}$ for the decay sequence $\frac{1}{2}(Q)\frac{3}{2}(Q+D)\frac{1}{2}$. The ordinate on the right is the ratio P of the linear polarization intensities as a function of δ for the decay sequence $\frac{1}{2}(Q)\frac{3}{2}(E2+M1)\frac{1}{2}$.

[1] F. K. McGowan and P. H. Stelson, Phys. Rev. **106**, 522 (1957).
[2] Biedenharn, Goldstein, McHale, and Thaler, Phys. Rev. **101**, 662 (1956); K. Alder and A. Winther, Kgl. Danske Videnskab. Selskab, Mat.-fys. Medd. **29**, No. 19 (1955).
[3] L. C. Biedenharn and M. E. Rose, Revs. Modern Phys. **25**, 729 (1953).

TABLE I. Targets and method of preparation.

Target	Isotopic abundance[a]	Method of preparation	Remarks
Ti^{205}	95.2%	electrodeposition	Thallium perchlorate bath
Tl^{203}	61.0	electrodeposition	Thallium perchlorate bath
Au^{197}	100	electrodeposition	Gold cyanide bath
Ir^{193}	89.14	sintered	
Re^{187}	62.93	sintered	Metallic powder obtained from a deposit of Re electrodeposited from a rhenium sulfate bath.
Re^{185}	85.38	sintered	
W^{183}	82.0	sintered	Metallic powder obtained from the reduction of the oxide in H_2 at an elevated temperature.
Ta^{181}	100	commercial foil	0.003 inch thick
Cd^{113}	54.1	electrodeposition	Cadmium cyanide bath
Cd^{111}	64.5	electrodeposition	Cadmium cyanide bath
Ag^{109}	98.4	electrodeposition	Silver cyanide bath
Ag^{107}	95.7	electrodeposition	Silver cyanide bath
Rh^{103}	100	commercial foil	0.002 inch thick
Mo^{95}	91.27	sintered	Metallic powder obtained from the reduction of the oxide in H_2 at an elevated temperature.

[a] The enriched isotopes and the isotopic analysis were supplied by the Stable Isotopes Research and Production Division at ORNL.

has been determined by measurements of the known polarization of gamma rays from Coulomb-excitation of 2+ levels in even-even nuclei.

We wish to report measurements of the yields, angular distributions, and polarization of gamma rays following Coulomb excitation. Polarization-direction measurements[4] of several transitions have resolved the ambiguity either in the value of $(E2/M1)^{\frac{1}{2}}$ or for the spin of the excited state. Reduced transition probabilities are obtained and in some instances these quantities are compared to the predictions of the collective model.[5]

II. APPARATUS

Protons and singly and doubly ionized He ions of variable energy were obtained from the 5.5-million volt ORNL Van de Graaff accelerator. Metallic targets were prepared either by electrodeposition onto 0.005-inch Ni or by sintering metallic powders into thin foils 0.5 inch in diameter by 75 to 150 mg/cm² thick. In Table I we have listed the targets and the method of preparation. For the electrodeposition of thallium, peptone and cresylic acid were used as additives[6] to prevent formation of Tl_2O_3 at the platinum anode and to reduce crystalline thallium at the cathode. In general we find that targets prepared by electrodeposition are relatively free of light-element impurities which are very troublesome in Coulomb-excitation experiments. The target support arrangement and methods of measuring yields and angular distributions have already been described.[7,1]

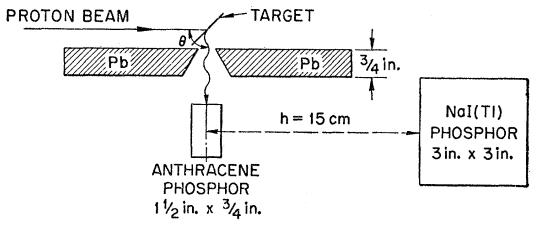

FIG. 2. Cross section through the gamma-ray polarimeter in the plane defined by the proton beam and the direction of propagation of the gamma ray.

A cross section through the γ-ray polarimeter in the plane defined by the ion beam and the direction of propagation of the gamma ray is shown in Fig. 2. The anthracene scatterer and the 3×3-in. NaI crystal which are connected to photomultiplier tubes constitute the polarization-sensitive device. The NaI scintillation spectrometer detects the radiation scattered through a mean angle of 90° and the anthracene scintillation spectrometer detects the Compton recoil electron. The detector of the scattered radiation rotates about an axis passing through the scatterer and the target. One measures $N_{\parallel}/N_{\perp}$, the ratio of the coincidence rate for the detector of the Compton-scattered photon in the plane of the proton beam and the gamma ray to the coincidence rate for the perpendicular position. This ratio is connected to the ratio of linear polarization intensities of the incident gamma ray through the relation

$$N_{\parallel}/N_{\perp}=(P+R)/(PR+1),$$

where R is the sensitivity of the polarimeter. For ideal geometry, R is simply the ratio of the differential

[4] A brief account of some of these measurements was presented at the 1956 Washington Meeting of the American Physical Society, P. H. Stelson and F. K. McGowan, Bull. Am. Phys. Soc. Ser. II, 1, 164 (1956).

[5] A. Bohr and B. Mottelson, Kgl. Danske Videnskab. Selskab, Mat.-fys. Medd. 27, No. 16 (1953).

[6] O. W. Brown and A. McGlynn, Trans. Am. Electrochem. Soc. 53, 351 (1928).

[7] P. H. Stelson and F. K. McGowan (to be published).

TABLE II. Summary of transitions used to calibrate polarimeter.

Nucleus	E_γ (kev)	E_p (Mev)	Transition	Character	$P(\theta=\frac{1}{2}\pi)$	$(N_{\text{II}}/N_\perp)_{\text{exp}}$	R
$Os^{190,192}$	186 206	3.0	$2\rightarrow 0$	$E2$	2.030	0.578±0.008	8.4±1.0
Pt^{194}	330	4.0	$2\rightarrow 0$	$E2$	2.173	0.566±0.008	7.0±1.0
Rh^{103}	360	2.7	$\frac{5}{2}\rightarrow\frac{1}{2}$	$E2$	2.071	0.607±0.012	5.7±0.6
Pd^{110}	374	2.7	$2\rightarrow 0$	$E2$	2.605	0.524±0.008	5.7±0.4
$Ag^{107,109}$	420	2.7	$\frac{5}{2}\rightarrow\frac{1}{2}$	$E2$	2.230	0.607±0.013	4.6±0.5
Pd^{108}	433	3.0	$2\rightarrow 0$	$E2$	2.607	0.550±0.016	4.7±0.5

Compton cross section averaged over the polarizations of the scattered photon, i.e., $R=(d\sigma/d\Omega)_{\beta=\pi/2}/(d\sigma/d\Omega)_{\beta=0}$ and β is the angle between direction of polarization of the incident photon and the plane of scattering. The finite extent of the detectors reduces the value of the asymmetry ratio R.

The resolving time 2τ of the fast-slow coincidence system was 0.25 μsec. A single-channel analyzer with a window width of approximately 30 kev selected the Compton recoil electrons. The coincidence rate was displayed as a pulse-height spectrum of the Compton-scattered gamma rays in 20 channels of a 20- by 120-channel analyzer[8] which was gated by the output of the fast-slow coincidence system. To assure that the axis of rotation of the detector passed through the target, the following alignment procedure was used. First, the location of the proton beam on the target was determined. Then a source of either Cr^{51}(320 kev) or Hg^{203}(279 kev) of the same area as the beam was placed on the target at this position. The axis of rotation was adjusted until the coincidence counting rates showed that $N_{\text{II}}/N_\perp$ did not differ from unity by more than 0.5%. A typical spectrum of the scattered radiation in coincidence with the Compton recoil electron is shown in Fig. 3 for 279-kev gamma rays from a Hg^{203} source incident on the scatterer. A sum of the counts in an appropriate number of channels was taken as a measure of N_{II} and $N_\perp$.

The asymmetry ratio R for our polarimeter was determined by measurement of the known polarization of gamma rays having pure multipole character for which the spins of the levels were known. In Table II we tabulate transitions following Coulomb excitation that were used to calibrate the polarimeter. The values for P are those for a thick target. A pulse-height spectrum of the scattered radiation for the 330-kev gamma radiation following Coulomb excitation in Pt^{194} incident on the polarimeter is also shown in Fig. 3. In all cases the intensities N_{II} and $N_\perp$ have been corrected for the bremsstrahlung continuum which is weak compared to the nuclear gamma intensity. For polarization-direction measurements with $Z\gtrsim 76$ a Bi target was used, and for measurements with Z of 42 to 48 a Sn target was used. The asymmetry in the polarization-direction correlation of the bremsstrahlung was large, i.e., $(P-1)>0$. The values obtained for the asymmetry ratio R of the polarimeter are also shown in Fig. 4 as a function of the gamma-ray energy and may be compared with those for ideal geometry. The calibration could have been extended to larger gamma-ray energies by using the radiation from Coulomb excitation of 2+ states in other suitable even-even nuclei of medium weight. This extension of the calibration was not needed for the experiments to be discussed in this paper. In any case Coulomb excitation affords an easy and rapid means of calibrating a polarimeter.

III. MEASUREMENTS

A. Gamma-Ray Yields

Figures 5 to 12 show pulse-height spectra of gamma radiation observed when thick targets of Tl^{205}, Tl^{203},

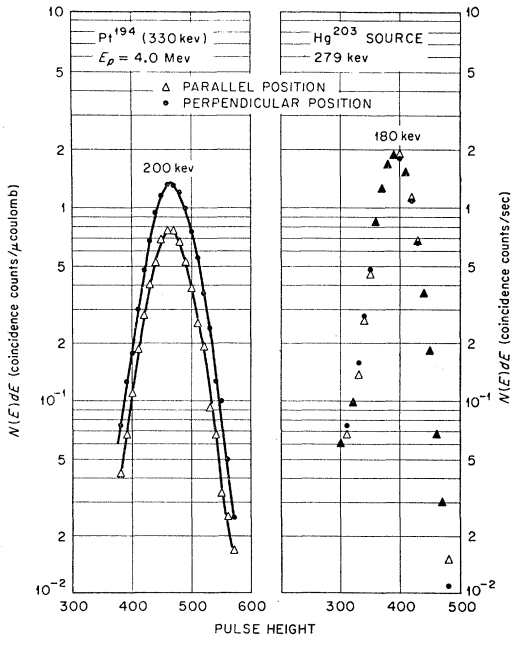

FIG. 3. Differential pulse-height spectrum of the radiation scattered through mean angle of 90° in coincidence with the Compton recoil electron. On the right is the spectrum when 279-kev gamma rays from a source of Hg^{203} are incident on the scatterer. On the left is the spectrum when 330-kev gamma rays following Coulomb excitation in Pt^{194} are incident on the scatterer.

[8] Kelley, Bell, and Goss, Oak Ridge National Laboratory Physics Division Quarterly Progress Report ORNL-1278, 1951 (unpublished).

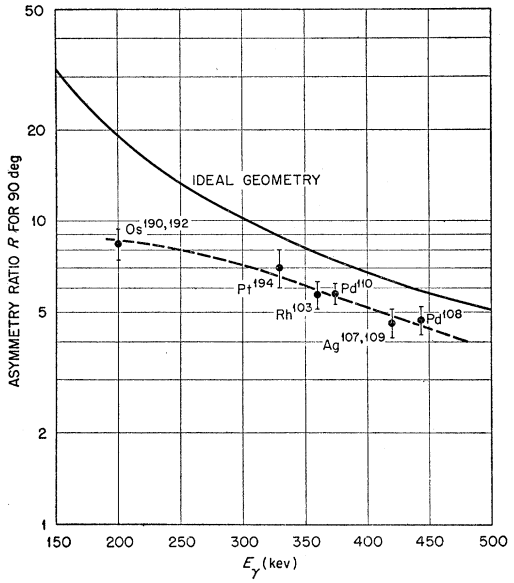

FIG. 4. Asymmetry ratio R as a function of E_γ for both ideal and finite geometry at a mean scattering angle of 90 degrees.

Ir^{193}, Re^{185}, W^{183}, Cd^{113}, Cd^{111}, and Mo^{95} were bombarded by protons. The spectrum of the accompanying proton bremsstrahlung continuum and local background is also shown. The shape of the pulse-height spectrum for each gamma ray of discrete energy is indicated in each figure. Pulse heights were converted to gamma-ray energies by measuring the spectra from radioactive sources which emit gamma rays of well-established energies. It was found that the DuMont photomultiplier tubes exhibit small shifts in pulse height for sources of different strength and for this reason we measured the spectrum of the gamma rays from Coulomb excitation and from radioactive sources simultaneously.

The gamma rays we have observed when the indicated nuclei were bombarded by protons and α particles are listed in Table III. The thick-target yield of gamma

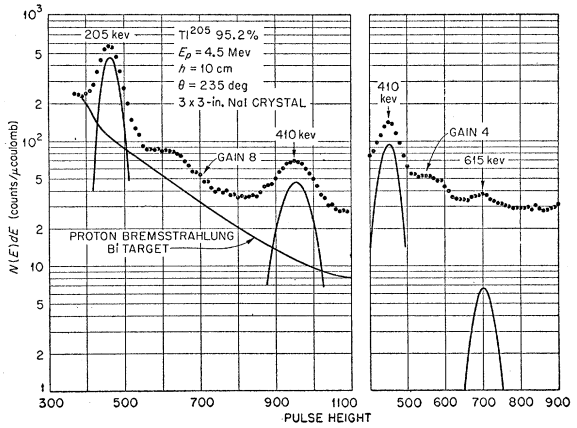

FIG. 5. Differential pulse-height spectrum of the gamma radiation for proton bombardment of Tl^{205}.

rays for an incident energy E_i is given in column 6 and the last column gives the numerical evaluation of the integral

$$\int_0^{E_i} \frac{g_2(\xi,\eta_i)E'dE}{dE/d\rho x}$$

in units of kev×mg/cm². $E'=k^2[E-\Delta E/k]$, where k is M_2/M_1+M_2 and M_1 and M_2 are the masses of the projectile and target nuclei, respectively, E is the exciting particle energy in the laboratory system, ΔE is the energy of the excited state above the ground state, and $dE/d\rho x$ is the rate of energy loss of the projectile in the target. The excitation function $g_2(\xi,\eta_i)$ for electric quadrupole excitation has been accurately evaluated.[2,9]

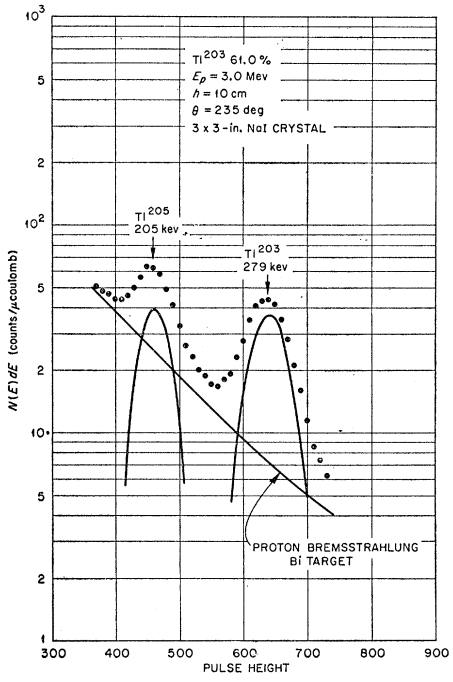

FIG. 6. Differential pulse-height spectrum of the gamma radiation for proton bombardment of Tl^{203}.

The variables ξ and η_i are defined as

$$\xi=\frac{Z_1Z_2e^2}{h}\left(\frac{1}{v_f}-\frac{1}{v_i}\right) \quad \text{and} \quad \eta_i=\frac{Z_1Z_2e^2}{hv_i},$$

where Z_1e and Z_2e are the charges of the impinging projectile and the nucleus, respectively, and v_i and v_f are the initial and final relative velocities.

B. Angular Distribution

Angular distributions have been measured for the gamma rays following Coulomb excitation in Tl^{205}, Tl^{203}, Au^{197}, Ir^{193}, Ir^{191}, Re^{187}, Re^{185}, Ta^{181}, Cd^{113}, Cd^{111},

[9] See, for instance, the review paper by Alder, Bohr, Huus, and Winther, Revs. Modern Phys. 28, 432 (1956).

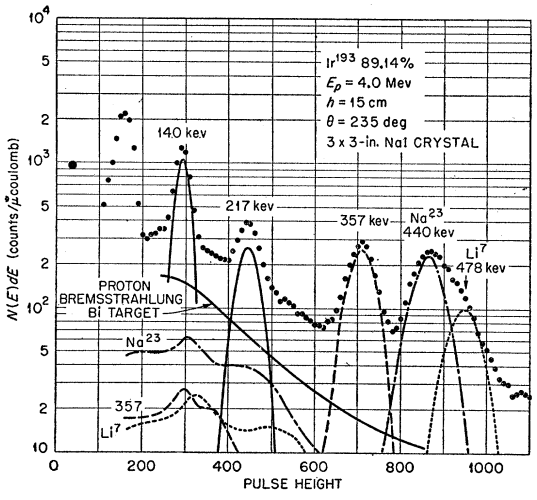

FIG. 7. Differential pulse-height spectrum of the gamma radiation for proton bombardment of Ir^{193}.

Ag^{109}, Ag^{107}, Rh^{103}, and Mo^{95}. In Table IV we list the observed angular distribution coefficients $(a_\nu G_\nu A_\nu)_{\text{exp}}$ which have been corrected for finite angular resolution. The errors quoted for these coefficients in Table IV include the standard deviation to be expected from the finite number of counts collected in the experiment and a decentering error.

C. Polarization-Direction Correlations

A number of the angular distribution measurements in Table IV could be fitted equally well either by two rather different values of $(E2/M1)^{\frac{1}{2}}$ or by two different spins for the excited state. Polarization-direction correlation measurements of transitions in Tl^{205}, Tl^{203}, Au^{197}, Cd^{113}, Cd^{111}, Ag^{109}, Ag^{107}, Rh^{103}, and Mo^{95} have removed the ambiguity. The results of these measurements are summarized in Table V.

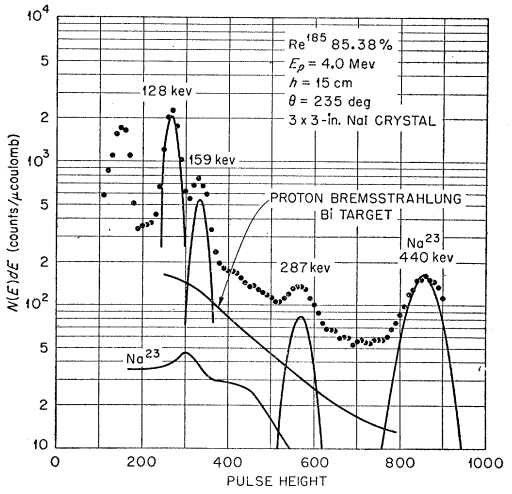

FIG. 8. Differential pulse-height spectrum of the gamma radiation for proton bombardment of Re^{185}.

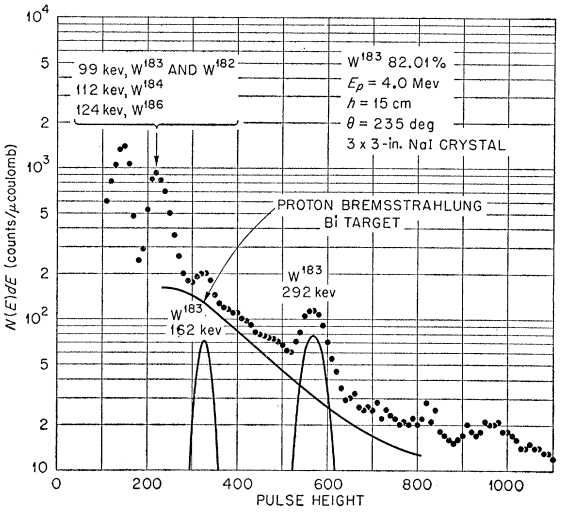

FIG. 9. Differential pulse-height spectrum of the gamma radiation for proton bombardment of W^{183}.

IV. INTERPRETATION AND DISCUSSION

In order to deduce the A_ν from the measured angular distribution coefficients, we must evaluate the expected thick-target particle parameters. These particle parameters for a thick target have been evaluated for a number of specific cases.[1] The attenuation coefficients G_ν, resulting from the slight attenuation of the angular distribution of the gamma rays by the multiple scattering of the protons by Rutherford scattering as they traverse a thick target, have been discussed in a previous paper.[1] In that paper the effective attenuation coefficient $[G_\nu]_t$ was defined as

$$[G_\nu]_t=[a_\nu G_\nu]_t/[a_\nu]_t.$$

We have found it useful to plot $[a_\nu]_t \times [G_\nu]_t$ as a func-

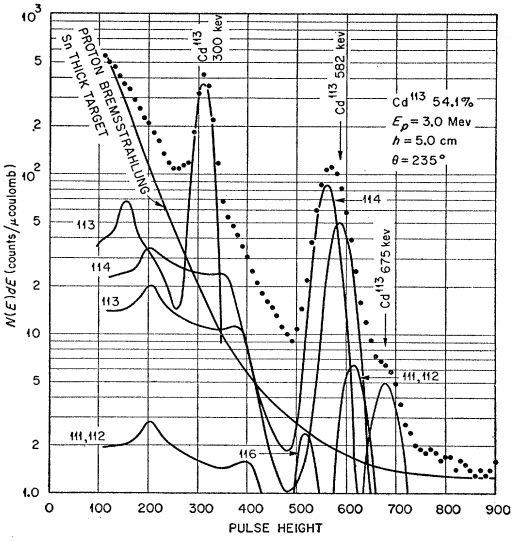

FIG. 10. Differential pulse-height spectrum of the gamma radiation for proton bombardment of Cd^{113}.

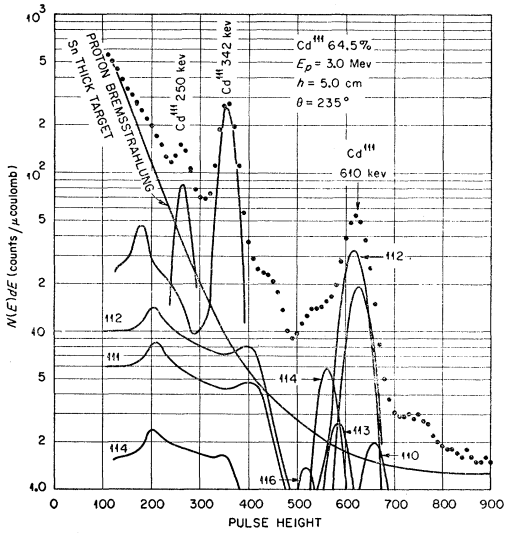

FIG. 11. Differential pulse-height spectrum of the gamma radiation for proton bombardment of Cd^{111}.

tion of ξ, where the variable ξ is evaluated for a projectile energy E_i, corresponding to the incident proton energy on the thick target.

Curves for a number of specific cases are given in Figs. 13 and 14. Instead of computing the thick-target parameters for all the individual cases, it was found that interpolation of these curves resulted in sufficiently accurate values for $[a_\nu]_t \times [G_\nu]_t$. These values are listed in Table IV under the column headed $(a_2G_2)_t$. In general the coefficient of $P_4(\cos\theta)$ is small and is not used in deducing the spins or $(E2/M1)^{\frac{1}{2}}$. The transition assignment and $(E2/M1)^{\frac{1}{2}}$ are obtained from $(A_2)_{\text{exp}}$. For those cases, where A_4 is large in magnitude, the sign of $(a_4G_4A_4)_{\text{exp}}$ is consistent with the assignment given in Table IV.

The reduced transition probabilities are obtained from the gamma-ray yields and the semiclassical expression of Alder and Winther[10] for the cross section for electric quadrupole excitation. The thick-target yield is related to $B(E2)_{\text{exc}}$ by the expression

$$\frac{B(E2)_{\text{exc}}}{e^2} = 7.01\times10^{-56}\frac{A_2Z_2^2}{m_1}\frac{I}{\int_0^{E_i}\frac{g_2(\xi,\eta_i)E'dE}{dE/d\rho x}}, \quad (1)$$

where A_2 is the atomic weight of the normal element, m_1 is the mass of the incident bombarding particle in units of the nucleon mass, and I is the number of excitations per microcoulomb of singly ionized particles. The $B(E2)$ for decay is obtained from the $B(E2)$ for excitation by multiplication by the factor $(2I_0+1)/(2I+1)$ where I_0 and I are spins of the ground state and the excited state, respectively.

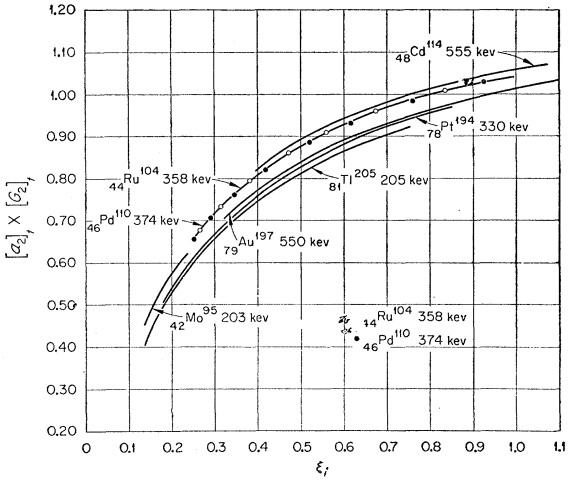

FIG. 13. Thick-target particle parameter $[a_2]_t \times [G_2]_t$ for protons as a function of ξ for a few representative cases.

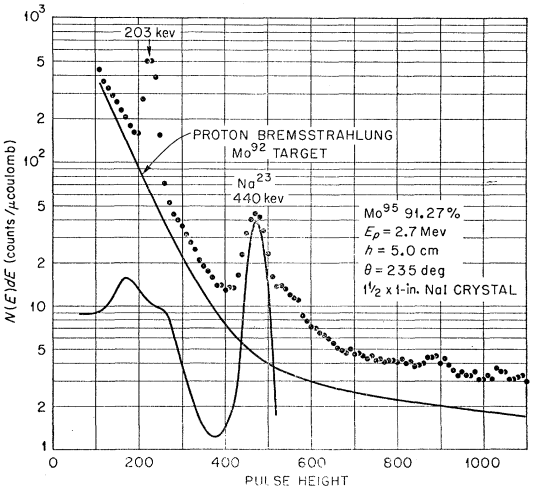

FIG. 12. Differential pulse-height spectrum of the gamma radiation for proton bombardment of Mo^{95}.

The total internal conversion coefficient α_T must be known in order to relate the cross sections to the observed gamma-ray yields. For this purpose the calculations of K-shell conversion coefficients by Rose *et al.*[11] have been used. Where the effect of the finite size of the nucleus is important, we have used the calculations by Sliv.[12] For the L and M shells, the K/L and L/M ratios by Rose[13] have been used. In the case of mixed $M1$-$E2$ transitions, it was necessary to use the $E2/M1$ ratio to obtain α_T.

To avoid confusion the reduced transition probabilities for excitation and decay will be written as $B(E2)_{\text{exc}}$ and $B(E2)_d$. In those cases, where the ratio

[10] K. Alder and A. Winther, Phys. Rev. **96**, 237 (1954).
[11] Rose, Goertzel, Spinrad, Harr, and Strong, Phys. Rev. **83**, 79 (1951).
[12] L. A. Sliv and I. M. Band, "Coefficients of internal conversion of gamma radiation, Part I: K-Shell," Acad. Sci. U.S.S.R. (1956) (Translation: University of Illinois Report 57ICCK1).
[13] "Tables of Internal Conversion Coefficients" (privately circulated by M. E. Rose).

TABLE III. Gamma rays observed when the listed nucleus was bombarded by protons and/or α particles. The column headed E gives the incident particle energy in Mev. The thick-target yield of gamma rays for an incident particle energy E_i is given in column 6. The last column gives the evaluation of the integral $\int_0^{E_i} g_2(\xi,\eta_i)E'dE/dE/d\rho x$ in units of kev×mg/cm².

Nucleus	Bombarding particle	E (Mev)	E_γ (kev)	E_i (Mev)	Yield of γ rays per μcoulomb	$\int_0^{E_i} \frac{g_2(\xi,\eta_i)E'dE}{dE/d\rho x}$
Tl^{205}	p	3.0 to 4.5	205±2	3.0	(2.52±0.20)×10⁴	3.85×10⁴
	p	3.0 to 4.5	410±4	4.5	(3.21±0.26)×10⁴	
	p	3.0 to 4.5	615±5	4.5	(4.1 ±1.2)×10³	3.52×10⁴
Tl^{203}	p	3.0 to 4.5	279±2	3.0	(2.34±0.23)×10⁴	2.30×10⁴
	p	3.0 to 4.5	403±5	4.5	(4.00±0.50)×10⁴	
Au^{197}	α	3.0 to 4.0	77	4.044	(1.56±0.40)×10⁴	1.17×10⁴
Ir^{193}	p	3.0 to 4.0	140±2	4.0	(5.68±0.40)×10⁵	1.57×10⁵
	p	3.0 to 4.0	217±2	4.0	(1.51±0.11)×10⁵	
	p	3.0 to 4.0	357±4	4.0	(2.63±0.18)×10⁵	6.68×10⁴
	α	3.0 to 4.0	140±2	4.044	(5.05±0.25)×10⁴	4.21×10³
Re^{187}	p	3.0 to 4.0	134±2	4.0	(1.13±0.10)×10⁶	1.59×10⁵
	p	3.0 to 4.0	167±2	4.0	(3.00±0.30)×10⁵	
	p	3.0 to 4.0	301±4	4.0	(5.2 ±1.3)×10⁴	8.72×10⁴
	α	3.0 to 4.0	134±2	4.044	(1.29±0.07)×10⁵	4.88×10³
Re^{185}	p	3.0 to 4.0	128±2	4.0	(1.26±0.10)×10⁶	1.61×10⁵
	p	3.0 to 4.0	159±2	4.0	(2.95±0.27)×10⁵	
	p	3.0 to 4.0	287±4	4.0	(6.6 ±1.7)×10⁴	9.21×10⁴
	α	3.0 to 4.0	128±2	4.044	(1.40±0.07)×10⁵	5.36×10³
W^{183}	p	4.0	99±2	4.0	(6.04±0.48)×10⁵	1.78×10⁵
	p	4.0	162±2	4.0	(3.8 ±0.4)×10⁴	
	p	4.0	292±3	4.0	(6.40±0.45)×10⁴	8.96×10⁴
Ta^{181}	α	3.0 to 4.0	136±2	4.044	(2.11±0.11)×10⁵	4.84×10³
Cd^{113}	p	2.1 to 3.3	300±3	3.0	(1.79±0.12)×10⁵	2.88×10⁴
	p	2.1 to 3.3	582±6	3.0	(1.07±0.11)×10⁵	6.36×10³
	p	2.1 to 3.3	675±7	3.0	(1.50±0.22)×10⁴	3.49×10³
Cd^{111}	p	2.1 to 3.3	250±3	3.0	(1.46±0.15)×10⁴	
	p	2.1 to 3.3	342±3	3.0	(1.40±0.09)×10⁵	2.37×10⁴
	p	2.1 to 3.3	610±6	3.0	(3.81±0.57)×10⁴	5.37×10³
Ag^{109}	p	3.0	107±2	3.0	(1.88±0.19)×10⁴	
	p	3.0	309±2	3.0	(4.38±0.24)×10⁵	2.81×10⁴
	p	3.0	416±3	3.0	(3.50±0.19)×10⁵	1.67×10⁴
Ag^{107}	p	3.0	99±2	3.0	(2.00±0.20)×10⁴	
	p	3.0	324±2	3.0	(3.81±0.21)×10⁵	2.62×10⁴
	p	3.0	423±3	3.0	(3.05±0.17)×10⁵	1.62×10⁴
Rh^{103}	p	3.0	62±2	3.0	(4.58±0.46)×10⁴	
	p	3.0	298±2	3.0	(5.20±0.29)×10⁵	3.02×10⁴
	p	3.0	360±3	3.0	(5.08±0.28)×10⁵	2.29×10⁴
Mo^{95}	p	1.8 to 3.0	203±2	2.7	(8.54±0.60)×10⁴	2.92×10⁴

$E2/M1$ is known, the reduced magnetic dipole transition probability for decay is obtained. These quantities are summarized in Table VI. The values given for $B(E2)$ and $B(M1)$ are actually those for the quantities $B(E2)/e^2$ and $B(M1)/(e\hbar/2mc)^2$. The error quoted for the $B(E2)_{\text{exc}}$ in Table VI is a standard deviation including the error from the gamma-ray yields and errors of ±4% for $dE/d\rho x$ and ±3% in the numerical evaluation of the integral in Eq. (1). We have omitted any possible uncertainty in α_T because such an error is difficult to assign. For instance, it is not clear whether internal conversion coefficients are independent of nuclear properties as was previously believed.[14] If the α_T should need to be changed, the reduced transition probabilities could be corrected accordingly from the information given in the tables.

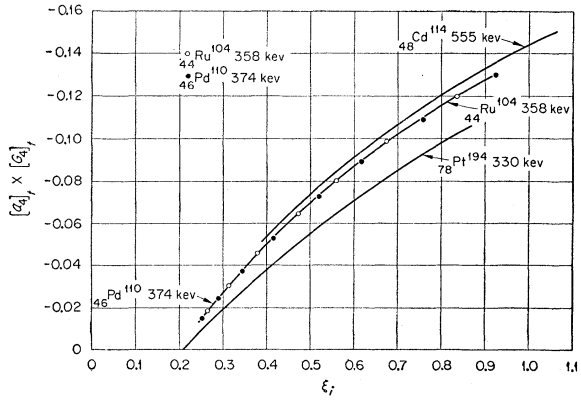

FIG. 14. Thick-target particle parameter $[a_4]_t \times [G_4]_t$ for protons as a function of ξ for a few representative cases.

It is of interest to compare the observed values of $B(E2)$ and $B(M1)$ to those expected for transitions between single-particle states of the independent-particle model. Using the estimate given by Blatt and Weisskopf,[15] one has that $B(M1)_{\text{sp}}$ is approximately unity and that $B(E2)_{\text{sp}}$ is given approximately by $(1/4\pi)|\frac{3}{5}R_0^2|^2$. We have taken R_0 equal to $1.2\times10^{-13}A^{\frac{1}{3}}$ cm.

[14] E. L. Church and J. Weneser, Phys. Rev. **104**, 1382 (1956).
[15] J. M. Blatt and V. F. Weisskopf, *Theoretical Nuclear Physics* (John Wiley and Sons, Inc., New York, 1952), Chap. XII.

TABLE IV. Proton-gamma angular distribution coefficients of the terms in the expansion of the correlation funtion in Legendre polynomials for a thick target.

Nucleus	E_p (Mev)	E_γ (kev)	Spin sequence	$(A_2)_{\gamma\gamma}$	$(a_2G_2A_2)_{\text{exp}}$	$(a_2G_2)_t$	$(A_2)_{\text{exp}}$	$\delta=(E2/M1)^{\frac{1}{2}}$	$(a_4G_4A_4)_{\text{exp}}$
$_{81}Tl^{205}$	3.0	205	$\frac{1}{2}(E2)\frac{3}{2}(E2+M1)\frac{1}{2}$		0.315±0.010	0.600	0.525±0.017	1.7±0.3	−(0.068±0.012)
	4.5	410	$\frac{1}{2}(E2)\frac{5}{2}(E2+M1)\frac{3}{2}$		−(0.18 ±0.02)	0.815	−(0.22 ±0.02)	≤-0.05	−(0.02 ±0.01)
$_{81}Tl^{203}$	3.0	279	$\frac{1}{2}(E2)\frac{3}{2}(E2+M1)\frac{1}{2}$		0.310±0.013	0.725	0.428±0.018	1.0 to 3.9	−(0.015±0.017)
	4.5	403	$\frac{1}{2}(E2)\frac{5}{2}(E2+M1)\frac{3}{2}$		−(0.14 ±0.02)	0.855	−(0.16 ±0.02)	≤0.05	−(0.03 ±0.02)
$_{79}Au^{197}$	3.0	277	$\frac{3}{2}(E2)\frac{5}{2}(E2+M1)\frac{3}{2}$		−(0.128±0.005)	0.704	−(0.182±0.007)	−(0.41±0.04)	−(0.006±0.005)
$_{77}Ir^{193}$	1.9	140	$\frac{3}{2}(E2)\frac{5}{2}(E2+M1)\frac{3}{2}$		−(0.143±0.014)	0.690	−(0.207±0.020)		0.0135±0.017
	2.4	140	$\frac{3}{2}(E2)\frac{5}{2}(E2+M1)\frac{3}{2}$		−(0.117±0.009)	0.570	−(0.204±0.014)	−(0.75±0.25)	−(0.038±0.010)
	2.7	140	$\frac{3}{2}(E2)\frac{5}{2}(E2+M1)\frac{3}{2}$		−(0.097±0.007)	0.520	−(0.187±0.014)		−(0.001±0.007)
	3.6	217	$\frac{3}{2}(E2)\frac{7}{2}(E2+M1)\frac{5}{2}$		−(0.239±0.019)	0.710	−(0.337±0.027)	−0.22 or	−(0.069±0.024)
	4.0	217	$\frac{3}{2}(E2)\frac{7}{2}(E2+M1)\frac{5}{2}$		−(0.205±0.005)	0.660	−(0.311±0.010)	−2.2	−(0.011±0.004)
	3.6	357	$\frac{3}{2}(E2)\frac{7}{2}(E2)\frac{3}{2}$	0.2186	0.157±0.006	0.710	0.221±0.010		0.010±0.006
	4.0	357	$\frac{3}{2}(E2)\frac{7}{2}(E2)\frac{3}{2}$	0.2186	0.139±0.006	0.660	0.211±0.010	∞	0.010±0.007
$_{77}Ir^{191}$	3.6	348	$\frac{3}{2}(E2)\frac{7}{2}(E2)\frac{3}{2}$	0.2186	0.150±0.010	0.700	0.214±0.014		−(0.019±0.012)
	4.0	348	$\frac{3}{2}(E2)\frac{7}{2}(E2)\frac{3}{2}$	0.2186	0.111±0.008	0.650	0.171±0.012	∞	−(0.011±0.008)
$_{75}Re^{187}$	3.6	167	$\frac{5}{2}(E2)\frac{9}{2}(E2+M1)\frac{7}{2}$		−(0.013±0.006)	0.63	∼0	0.16±0.04	0.070±0.007
	4.0	167	$\frac{5}{2}(E2)\frac{9}{2}(E2+M1)\frac{7}{2}$		−(0.038±0.011)	0.58	∼0	0.16±0.04	0.031±0.013
$_{75}Re^{185}$	3.6	159	$\frac{5}{2}(E2)\frac{9}{2}(E2+M1)\frac{7}{2}$		0.018±0.008	0.62	∼0	0.16±0.04	−(0.008±0.008)
$_{73}Ta^{181}$	4.0	166	$\frac{7}{2}(E2)1\frac{1}{2}(E2+M1)\frac{9}{2}$		0.121±0.009	0.584	0.208±0.015	0.50±0.04	0.024±0.012
$_{48}Cd^{113}$	2.1	300	$\frac{1}{2}(E2)\frac{3}{2}(E2+M1)\frac{1}{2}$		0.018±0.007	0.815	0.022±0.009	0.29 or	−(0.005±0.008)
	2.4	300	$\frac{1}{2}(E2)\frac{3}{2}(E2+M1)\frac{1}{2}$		0.012±0.007	0.750	0.016±0.009	−4.0	0.005±0.008
	3.0	582	$\frac{1}{2}(E2)\frac{5}{2}(E2)\frac{1}{2}$	0.2857	0.223±0.033	0.893	0.25 ±0.04		−(0.032±0.043)
	3.3	582	$\frac{1}{2}(E2)\frac{5}{2}(E2)\frac{1}{2}$	0.2857	0.218±0.023	0.840	0.26 ±0.03	∞	−(0.036±0.029)
$_{48}Cd^{111}$	2.1	342	$\frac{1}{2}(E2)\frac{3}{2}(E2+M1)\frac{1}{2}$		0.099±0.006	0.865	0.114±0.008	0.385 or	−(0.011±0.007)
	2.4	342	$\frac{1}{2}(E2)\frac{3}{2}(E2+M1)\frac{1}{2}$		0.077±0.005	0.800	0.096±0.006	−6.6	−(0.016±0.006)
	3.0	610	$\frac{1}{2}(E2)\frac{5}{2}(E2)\frac{1}{2}$	0.2857	0.17 ±0.03	0.910	0.19 ±0.04		−(0.031±0.025)
	3.3	610	$\frac{1}{2}(E2)\frac{5}{2}(E2)\frac{1}{2}$	0.2857	0.23 ±0.03	0.863	0.27 ±0.04	∞	−(0.066±0.028)
$_{47}Ag^{109}$	2.7	309	$\frac{1}{2}(E2)\frac{3}{2}(E2+M1)\frac{1}{2}$		−(0.268±0.005)	0.690	−(0.388±0.007)	−(0.19±0.01) or −1.15	0.010±0.005
$_{47}Ag^{107}$	2.7	324	$\frac{1}{2}(E2)\frac{3}{2}(E2+M1)\frac{1}{2}$		−(0.284±0.004)	0.705	−(0.403±0.006)	−(0.21±0.01) or −1.10	0.010±0.003
$_{45}Rh^{103}$	2.7	298	$\frac{1}{2}(E2)\frac{3}{2}(E2+M1)\frac{1}{2}$		−(0.251±0.004)	0.665	−(0.377±0.006)	−(0.17±0.01) or −1.2	0.009±0.003
$_{42}Mo^{95}$	2.4	203			−(0.073±0.006)	0.565	−(0.129±0.010)		0.005±0.006
	2.7	203			−(0.066±0.006)	0.506	−(0.130±0.012)		−(0.014±0.006)
	3.0	203			−(0.053±0.007)	0.451	−(0.118±0.016)		−(0.007±0.007)

TABLE V. Summary of transitions for which a polarization measurement has resolved the ambiguity either in the value of $(E2/M1)^{\frac{1}{2}}$ or for the spin of the excited state.

Nucleus	E_p (Mev)	E_γ (kev)	Transition	$(E2/M1)^{\frac{1}{2}}_{\text{ang. dist.}}$	$P(\theta=\pi/2)$	$P(\theta=\pi/2)_{\text{exp}}$	$(E2/M1)^{\frac{1}{2}}_{\text{polar.}}$
$_{81}Tl^{205}$	3.0	205	$\frac{3}{2}\rightarrow\frac{1}{2}$	1.7 ±0.3		0.91±0.06	1.46±0.16
$_{81}Tl^{203}$	3.0	279	$\frac{3}{2}\rightarrow\frac{1}{2}$	1.0 to 3.9		0.91±0.04	1.50±0.08
$_{79}Au^{197}$	3.0	277	$\frac{5}{2}\rightarrow\frac{3}{2}$	−(0.41±0.04)		1.00±0.02	−(0.53±0.08)
$_{48}Cd^{113}$	2.7	300	$\frac{3}{2}\rightarrow\frac{1}{2}$	0.29	0.54	0.61±0.03	
				−4.0	1.86		
$_{48}Cd^{111}$	2.7	342	$\frac{3}{2}\rightarrow\frac{1}{2}$	0.385	0.51	0.56±0.04	
				−6.6	1.97		
$_{47}Ag^{109}$	2.7	309	$\frac{3}{2}\rightarrow\frac{1}{2}$	−0.19	0.72	0.73±0.03	
				−1.15	1.39		
$_{47}Ag^{107}$	2.7	324	$\frac{3}{2}\rightarrow\frac{1}{2}$	−0.21	0.72	0.78±0.03	
				−1.10	1.37		
$_{45}Rh^{103}$	2.7	298	$\frac{3}{2}\rightarrow\frac{1}{2}$	−0.17	0.72	0.79±0.03	
				−1.2	1.40		
$_{42}Mo^{95}$	2.7	203	$\frac{3}{2}\rightarrow\frac{5}{2}$	−0.5 to −0.13		1.17±0.04	−(0.58±0.20)

A. Thallium

The angular distribution measurements of the 205-kev and 279-kev transitions in Tl^{205} and Tl^{203} did not provide a very precise measure of $\delta=(E2/M1)^{\frac{1}{2}}$. The large uncertainty results from the fact that A_2 has a broad maximum near $\delta=1.7$ (see Fig. 1). However, the ratio P of the linear polarization intensities is quite sensitive to small changes in δ for δ near to 1.7. As a result the values for δ in Table VI were obtained from the polarization-direction correlation measurements.

Extensive measurements of the internal conversion coefficients of the 279-kev transition in Tl^{203} have been made by several groups of workers.[16] From consistency arguments based on a comparison of the experimental values for α^K, α^{L_I}, $\alpha^{L_{II}}$, and $\alpha^{L_{III}}$ and the calculated coefficients[11,13] they obtained a value of $E2/M1=1.38\pm0.25$ which is smaller than our value of 2.25 ± 0.25. However, a more recent analysis[17] of their data using the calculated coefficients by Sliv[12] gives better agreement but their value is still somewhat smaller than the result from Coulomb excitation.

In the interpretation of our original measurements on normal thallium the $B(E2)_d$ for 403-kev transition in Tl^{203} appeared to be unexpectedly large.[18] We had taken the $E2$ intensity comparable to the $M1$ intensity as indicated by the measured values of α^K and K/L.[19,20] However, when the effect of the finite size of the nucleus on the internal conversion coefficients is taken in account, the measured values indicate that the 403-kev transition is predominantly $M1$ radiation. This agrees with the results of our angular distribution measurements. The $B(E2)_d$ for the 410-kev and 403-kev transitions in Tl^{205} and Tl^{203} are now comparable to $B(E2)_{\text{sp}}$ and are in agreement with the observed trend of the $B(E2)$ with the approach to closed shells.

Lindqvist and Marklund[21] have concluded from a measurement of the gamma-gamma angular correlation of the 403–279-kev cascade following electron capture of Pb^{203} that the 403-kev transition is predominantly $M1$ radiation. Unfortunately, their correlation measurement is very insensitive to the value of $E2/M1$ for the 279-kev transition.

The $M1$ transition probabilities in Tl^{203} and Tl^{205} can probably be understood qualitatively in terms of the nuclear shell-model. If one labels the $\frac{3}{2}\rightarrow\frac{1}{2}$ transitions as $d_{\frac{3}{2}}\rightarrow s_{\frac{1}{2}}$ transitions, the $M1$ radiation is forbidden according to the simple single-particle shell model by the l-selection rule, namely, transitions for which $\Delta l\neq 0$ are forbidden. Indeed, the $B(M1)_d$ for the 205- and 279-kev transitions are observed to be quite small compared to $B(M1)_{\text{sp}}$. In addition, decay by $E2$ radiation should compete favorably and the experimental results indicate this to be the case. The cascade transitions of 410- and 403-kev transitions in Tl^{205} and Tl^{203} would be labeled $d_{5/2}\rightarrow d_{\frac{3}{2}}$ and $M1$ radiation would be allowed. The transitions are observed to decay predominantly by $M1$ radiation and the $B(M1)_d$ are comparable to $B(M1)_{\text{sp}}$.

For the 205- and 279-kev excitations Barloutaud *et al.*[22] give $\epsilon B(E2)_{\text{exc}}=(0.072 \text{ and } 0.086)\times10^{-48}$ cm^4. Our values are $(0.062 \text{ and } 0.10)\times10^{-48}$ cm^4.

B. Au^{197}

In agreement with the work of others,[23,24] we find direct excitation of the 77-kev state in Au^{197} by α-particle bombardment. Since the gamma radiation of this energy is obscured by the K x-rays of gold when observed with a scintillation spectrometer, we made a study of the yield of K x-rays resulting from stopping the α particles in the target.[25] From the composite peak

[16] A. H. Wapstra and G. J. Nijgh, Nuclear Phys. **1**, 245 (1956); Nordling, Siegbahn, Sokolowski, and Wapstra, Nuclear Phys. **1**, 326 (1956).
[17] A. H. Wapstra (private communication).
[18] P. H. Stelson and F. K. McGowan, Phys. Rev. **99**, 112 (1955).
[19] Wapstra, Maeder, Nijgh, and Ornstein, Physica **20**, 169 (1954).
[20] J. Varma, Phys. Rev. **94**, 1688 (1954).
[21] T. Lindqvist and I. Marklund, Nuclear Phys. **3**, 367 (1957).
[22] Barloutaud, Grjebine, and Riou, Physica **22**, 1129 (1956).
[23] N. P. Heydenburg and G. M. Temmer, Phys. Rev. **93**, 351 (1954).
[24] E. M. Bernstein and H. W. Lewis, Phys. Rev. **100**, 1345 (1955).
[25] F. K. McGowan and P. H. Stelson, Phys. Rev. **103**, 1133 (1956).

TABLE VI. Summary of quantities obtained from $B(E2)_{exc}$. The value of $B(E2)_d$ is given in column 5 for the downward transition listed in column 4. From the values for cascade/crossover, α_T, and $E2/M1$, the values of $T_{1/2}$ and $B(M1)_d$ are calculated. The ratio cascade/crossover is the ratio of total transitions by cascade to crossover. The last column lists the ratio of the observed $B(E2)_d$ to that expected for a transition between states of the independent-particle model.

Nucleus	E_γ (kev)	$B(E2)_{exc}\times10^{49}$	Transition	$B(E2)_d\times10^{49}$	$\left(\frac{\text{Cascade}}{\text{crossover}}\right)$	$(E2/M1)^{\frac{1}{2}}$	α_T	$T_{1/2}$ (sec)	$B(M1)_d$	$\frac{B(E2)_d}{B(E2)_{sp}}$
$_{81}Tl^{205}$	205	1.00±0.10 cm^4	$\frac{3}{2}\rightarrow\frac{1}{2}$	0.50 cm^4		1.46±0.16	0.62	1.32×10^{-9}	6.9×10^{-4}	7.0
	410		$\frac{5}{2}\rightarrow\frac{3}{2}$	≤0.06		−0.05	0.171		2.7×10^{-1}	≤0.8
	615	1.14±0.13	$\frac{3}{2}\rightarrow\frac{1}{2}$	0.38	9	∞	0.019	1.66×10^{-12}		5.3
Tl^{203}	279	1.24±0.14	$\frac{3}{2}\rightarrow\frac{1}{2}$	0.62		1.50±0.08	0.246	3.00×10^{-10}	1.5×10^{-3}	8.7
	403		$\frac{5}{2}\rightarrow\frac{3}{2}$	≤0.12		0.05	0.176		5.5×10^{-1}	≤1.7
	682	2.10±0.27	$\frac{5}{2}\rightarrow\frac{1}{2}$	0.70	6	∞	0.015	0.77×10^{-12}		9.9
$_{79}Au^{197}$	277	3.35±0.27	$\frac{5}{2}\rightarrow\frac{3}{2}$	2.23		−(0.41±0.04)	0.38	1.62×10^{-11}	7.2×10^{-2}	33
$_{77}Ir^{193}$	140	7.44±0.67	$\frac{5}{2}\rightarrow\frac{3}{2}$	4.96		−(0.75±0.25)	1.94	2.59×10^{-10}	1.2×10^{-2}	74
	217		$\frac{7}{2}\rightarrow\frac{5}{2}$	1.00		−(0.22±0.03)	0.67		6.8×10^{-2}	15
	357	6.10±0.67	$\frac{7}{2}\rightarrow\frac{3}{2}$	3.05	0.93	∞	0.060	1.56×10^{-11}		46
$_{75}Re^{187}$	134	14.8 ±1.5	$\frac{7}{2}\rightarrow\frac{5}{2}$	11.1			(2.30)		(5.5×10^{-1})	175
	167		$\frac{9}{2}\rightarrow\frac{7}{2}$	9.98		0.16±0.04	1.21		7.6×10^{-1}	157
	301	6.45±0.71	$\frac{9}{2}\rightarrow\frac{5}{2}$	3.87	11	∞	0.090	4.52×10^{-12}		61
Re^{185}	128	18.7 ±1.8	$\frac{7}{2}\rightarrow\frac{5}{2}$	14.0			(2.58)		(6.3×10^{-1})	224
	159		$\frac{9}{2}\rightarrow\frac{7}{2}$	9.73		0.16±0.04	1.39		6.7×10^{-1}	155
	287	6.67±0.67	$\frac{9}{2}\rightarrow\frac{5}{2}$	4.00	11	∞	0.104	5.48×10^{-12}		64
$_{74}W^{183}$	99	27.1 ±3.0	$\frac{5}{2}\rightarrow\frac{1}{2}$	9.0		∞	4.0			146
	292	2.46±0.22	$\frac{5}{2}\rightarrow\frac{1}{2}$	0.82		∞	0.095			13
	209	0.49±0.06	$\frac{3}{2}\rightarrow\frac{1}{2}$	0.25						4
$_{73}Ta^{181}$	136	20.4 ±1.6	$\frac{9}{2}\rightarrow\frac{7}{2}$	16.3		0.5 ±0.05	1.53	5.68×10^{-11}	8.6×10^{-2}	270
	166		$1\frac{1}{2}\rightarrow\frac{9}{2}$	25.0		0.5 ±0.04	0.79		1.9×10^{-1}	412
	303	5.45±0.44	$1\frac{1}{2}\rightarrow\frac{7}{2}$	3.63	2.82	∞	0.079	1.48×10^{-11}		59
$_{48}Cd^{113}$	300	1.10±0.09	$\frac{3}{2}\rightarrow\frac{1}{2}$	0.55		0.29±0.01	0.026	3.20×10^{-11}	4.14×10^{-2}	18
	582	3.04±0.33	$\frac{5}{2}\rightarrow\frac{1}{2}$	1.01	0.02	∞	0.0044	9.05×10^{-1}		31
	675	0.9 ±0.14	$?\rightarrow\frac{1}{2}$		0.19					
$_{48}Cd^{111}$	342	1.10±0.09	$\frac{3}{2}\rightarrow\frac{1}{2}$	0.55	0.026	0.39±0.02	0.0184	2.72×10^{-11}	2.99×10^{-2}	18
	610	1.43±0.22	$\frac{5}{2}\rightarrow\frac{1}{2}$	0.48	0.29	∞	0.0039	1.08×10^{-11}		15
$_{47}Ag^{109}$	309	2.49±0.17	$\frac{3}{2}\rightarrow\frac{1}{2}$	1.25		−(0.19±0.01)	0.022	5.65×10^{-12}	2.25×10^{-1}	41
	107		$\frac{5}{2}\rightarrow\frac{3}{2}$			∼0	0.38		4.6×10^{-2}	
	416	3.77±0.26	$\frac{5}{2}\rightarrow\frac{1}{2}$	1.26	0.07	∞	0.0114	3.33×10^{-11}		41
Ag^{107}	324	2.19±0.15	$\frac{3}{2}\rightarrow\frac{1}{2}$	1.10		−(0.21±0.01)	0.020	5.93×10^{-12}	1.85×10^{-1}	36
	99		$\frac{5}{2}\rightarrow\frac{3}{2}$			∼0	0.47		7.7×10^{-2}	
	423	3.34±0.23	$\frac{5}{2}\rightarrow\frac{1}{2}$	1.11	0.10	∞	0.0108	3.38×10^{-11}		36
$_{45}Rh^{103}$	298	2.09±0.15	$\frac{3}{2}\rightarrow\frac{1}{2}$	1.05		−(0.17±0.01)	0.020	6.29×10^{-12}	2.27×10^{-1}	35
	62		$\frac{5}{2}\rightarrow\frac{3}{2}$			∼0	1.16		2.1×10^{-1}	
	360	3.93±0.28	$\frac{5}{2}\rightarrow\frac{1}{2}$	1.31	0.19	∞	0.0165	5.9×10^{-11}		45
$_{42}Mo^{95}$	203	0.35±0.03	$\frac{5}{2}\rightarrow\frac{5}{2}$	0.53		−(0.6 ±0.2)	0.054	7.64×10^{-10}	4.4×10^{-3}	21
$_{76}Os^{192}$	206	20.5 ±2.1	$2\rightarrow0$	4.1		∞	0.313	2.83×10^{-10}		62
Os^{190}	186	25.5 ±2.6	$2\rightarrow0$	5.1		∞	0.434	3.47×10^{-10}		79
Os^{188}	155	28.0 ±3.1	$2\rightarrow0$	5.6		∞	0.82	6.20×10^{-10}		88
$_{74}W^{186}$	124	35.6 ±3.6	$2\rightarrow0$	7.12		∞	1.75	9.85×10^{-10}		113
W^{184}	112	43.7 ±4.4	$2\rightarrow0$	8.74		∞	2.59	1.02×10^{-9}		141
W^{182}	100	44.7 ±5.4	$2\rightarrow0$	8.94		∞	3.98	1.27×10^{-9}		146

in the pulse-height spectrum, we have been able to obtain the yield of 77-kev gamma rays. We previously reported that we were unable to detect direct excitation of the 77-kev state.[18] The previously determined upper limit for the $B(E2)_{\text{exc}}$ is consistent with the new positive result.

Other information is available on the 77-kev transition. (a) Mihelich and de-Shalit[26] have measured the relative values of α^{L_I}, $\alpha^{L_{II}}$, and $\alpha^{L_{III}}$. From a comparison of these values with calculated values for $E2$ and $M1$ transitions one can deduce a value for $E2/M1$. (b) Sunyar[27] has measured the half-life of the state by the delayed coincidence method. (c) Bernstein and Lewis have measured the Coulomb excitation cross section by the detection of internal conversion electrons. From the comparison of the Coulomb excitation cross section and the half-life, Bernstein and Lewis concluded that the spin of the 77-kev state is $\frac{1}{2}$. However, this conclusion depends rather sensitively on the values for $E2/M1$ and α_T. They used the values $E2/M1=1/7$ and $\alpha_T=3.5$. With these values one deduces from the half-life that $B(E2)_{\text{exc}}$ is either 0.15 or 0.30×10^{-48} cm^4 depending on whether the spin is $\frac{1}{2}$ or $\frac{3}{2}$. From Coulomb excitation Bernstein and Lewis obtained a $B(E2)_{\text{exc}}$ of 0.18 which indicated a spin of $\frac{1}{2}$. However, if one uses the recently available calculated values of L-shell internal conversion coefficients by Rose with the assumption that the L-shell conversion coefficients are reduced by a factor equal to that for the K shell for $M1$ transitions to account for the finite nuclear-size effect to deduce $E2/M1$ and α_T from the experimental results of Mihelich and de-Shalit, one finds the values $E2/M1=1/9$ and $\alpha_T=4.26$. Taking these values, our gamma-ray yield measurements indicate $B(E2)_{\text{exc}}=(0.14_{-0.04}{}^{+0.02})\times10^{-48}$ cm^4. The results of the lifetime measurement are altered to give $B(E2)_{\text{exc}}$ of either 0.105 or 0.21×10^{-48} cm^4 for spin $\frac{1}{2}$ or $\frac{3}{2}$, respectively. Our result favors the spin $\frac{1}{2}$ but the uncertainties in the quantities needed to draw this conclusion do not completely exclude the spin $\frac{3}{2}$. For the spin assignment of $\frac{1}{2}$ the $B(E2)_d/B(E2)_{\text{sp}}$ and the $B(M1)_d$ are 41 and 10^{-2} for the 77-kev state.

The value of δ for the 277-kev transition found in our original measurement of the angular distribution was $-(0.75\pm0.20)$.[28] This value was based on our empirical determination of the particle parameter a_2. When reinterpreted by the use of the quantum calculations of the particle parameter a_2, the result is $\delta=-(0.55\pm0.08)$. The polarization-direction correlation and the more recent angular distribution measurement give the result $\delta=-(0.41\pm0.04)$ and we consider this to be our best value. Kane and Frankel[29] have deduced an $E2/M1$ value of 0.12 ± 0.03 for the 277-kev transition from a gamma-gamma directional angular correlation measurement. Our value of $E2/M1=0.17\pm0.03$, although still somewhat higher, is in better agreement with their value than our previous result. The $B(M1)_d$ for the 277-kev transition is increased from 2.1 to 7.2×10^{-2} using the more recent results for $E2/M1$.

C. Iridium

Composite gamma rays of 133, 219, and 360-kev have been observed by Coulomb excitation on normal iridium.[30] Davis *et al.*[31] observed gamma rays of 143, 230, and 368 kev following Coulomb excitation in Ir^{193}. We observed direct excitation of levels at 140 and 357 kev in Ir^{193} and this is consistent with the results of Davis *et al.* However, our results for $B(E2)_{\text{exc}}$ of 7.4 and 6.1×10^{-49} cm^4 are considerably larger than their values of 5.3 and 3.2×10^{-49} cm^4. From the angular distribution of the 217-kev gamma rays we obtained $E2/M1=0.048$. In Table VI we have taken the smaller value of $(E2/M1)^{\frac{1}{2}}$ for the 217-Mev transition from Table IV. Although this choice is somewhat arbitrary, it is in accord with observations for the analogous transitions in Re^{187}, Re^{185}, and Ta^{181}. Using the observed intensity ratio of cascade to crossover for gamma rays and assuming that the collective model gives the ratio of the cascade to crossover for $E2$ transition probabilities correctly, Davis *et al.* obtained $E2/M1=0.3$. We do agree with regard to the ratio of cascade to crossover for gamma rays. The discrepancy for $E2/M1$ is probably caused by the fact that the excitation spectrum is not a pure rotational spectrum.

Except for the angular distribution measurements for the 348-kev gamma ray from Ir^{191}, we have withheld our other measurements on Ir^{191}. The excitation spectrum with protons and α particles appears to be more complicated than was observed in Ir^{193}. As a result we are making more measurements on this nucleus.

D. Rhenium

In agreement with others,[9,31,32] we observe gamma rays with energies of 134, 167, and 301 kev in Re^{187} and of 128, 159, and 287 kev in Re^{185}. These are interpreted to be the result of direct excitation of levels at 134 and 301 kev in Re^{187} and at 128 and 287 kev in Re^{185}.

The determination of the δ value from the angular distribution of the 134- and 128-kev gamma rays is unfavorable because the transition of the type $\frac{5}{2}(E2)\frac{7}{2}(E2+M1)\frac{5}{2}$ is nearly isotropic for small admixtures of $E2$ radiation ($|A_2|\leq0.02$). The angular distributions have been measured and they are found to be isotropic to within 2%. We have taken the transitions to be predominantly $M1$ radiation, in

[26] J. W. Mihelich and A. de-Shalit, Phys. Rev. **91**, 78 (1953).
[27] A. W. Sunyar, Phys. Rev. **98**, 653 (1955).
[28] F. K. McGowan and P. H. Stelson, Phys. Rev. **99**, 127 (1955).
[29] J. V. Kane and S. Frankel, Bull. Am. Phys. Soc. Ser. II, **1**, 171 (1956).
[30] G. M. Temmer and N. P. Heydenburg, Phys. Rev. **93**, 906 (1954).
[31] Davis, Divatia, Lind, and Moffat, Phys. Rev. **103**, 1801 (1956).
[32] Wolicki, Fagg, and Ceer, Phys. Rev. **100**, 1265(A) (1955).

agreement with a K/L measurement[33,34] of the 134-kev transition in Re^{187}, for purposes of obtaining α_T and the $B(E2)_{exc}$. From the theory of nuclear rotational states, as developed by Bohr and Mottelson,[5] it follows that $\delta_1/\delta_{21}=1.02$ for $I_0=\frac{5}{2}$, where the subscript 21 denotes the cascade transition from the second to the first rotational state and the subscript 1 denotes the transition from the first to the ground state. Using the δ_{21} as given by the angular distribution measurements, we would have $\delta_1=0.16$ which is in agreement with the observed isotropic distribution because for $\delta_1=0.16$ the coefficient A_2 is equal to -0.002. The $B(M1)$ given in Table VI for the 134- and 128-kev transitions in Re^{187} and Re^{185} are based on this indirect determination of δ_1. The determination of the angular distribution of the 301-kev γ rays in Re^{187} was difficult because this crossover transition is relatively weak. Although the results are not very precise, the observed angular distribution is consistent with a transition assignment of $9/2(E2)\frac{5}{2}$.

E. Tungsten

Other workers[9] have found, by the use of enriched isotopes, gamma rays of 100-, 112-, and 124-kev energy resulting from Coulomb excitation of 2+ states in W^{182}, W^{184}, and W^{186}. In addition gamma rays of 46 and 99 kev are known[31] to follow Coulomb excitation in W^{183}. The energy levels in W^{183} have been very accurately determined up to an energy of 450 kev from a study of the gamma transitions following the β^- decay of Ta^{183} by Murray *et al.*[35] A γ ray of 295-kev energy was observed in our earlier measurements on normal tungsten and this was attributed to the Coulomb excitation of a state of this energy in W^{183}.

We have made additional studies of Coulomb excitation in tungsten using enriched isotopes W^{183}, W^{184}, and W^{186} and normal tungsten. The $B(E2)_{exc}$ and $B(E2)_d$ for the even-even isotopes are given in Table VI. The half-life of the 100-kev transition in W^{182} deduced from Coulomb excitation measurements is in good agreement with the direct measurement (1.27×10^{-9} sec) by Sunyar.[36]

For the enriched W^{183} target and incident proton energy of 4.0 Mev we observed the pulse-height spectrum shown in Fig. 9. In addition to the 99- and 292-kev gamma rays a gamma ray of 162 kev is also observed. We also observed three γ rays when W^{183} was bombarded with 10-Mev α particles. These gamma rays of 99-, 162-, and 292-kev energy are attributed to direct excitation of levels in W^{183} at 99, 209, and 292-kev. An energy level diagram of the low-lying levels in W^{183} as suggested by Murray *et al.*[35] and modified slightly by Kerman[37] is shown in Fig. 15. The deviation of the level pattern from that for a pure rotational band cannot be accounted for in terms of a rotation-vibration interaction. Kerman has been able to account for the deviations by the inclusion of a rotation-particle coupling acting between the ground-state band with $K=\frac{1}{2}^-$ and the first excited band with $K=\frac{3}{2}^-$. The transition probabilities for transitions between the two bands are predicted to be influenced in an important way by the inclusion of the rotation-particle coupling. The reduced transition probabilities calculated by Kerman using an intrinsic quadrupole moment $Q_0=6.5\times10^{-24}$ cm^2, which is consistent with values in neighboring nuclei, are also given in Fig. 15. For comparison the observed values are given in Fig. 15. The agreement between theory and experiment is good in view of the uncertainty in the total internal conversion coefficients and the branching ratios from the decay scheme of Murray *et al.* According to Kerman the $B(E2)_{exc}$ for excitation in the $K=\frac{3}{2}^-$ band would be reduced by more than a factor of ten without the rotational admixture. Using the decay scheme and branching ratios by Murray *et al.* we have obtained the $B(M1)_d$ for several transitions given in Fig. 15.

F. Ta^{181}

No additional measurements on Ta^{181} have been made except for the angular distribution measurement of the 166-Mev gamma rays. The value of $(E2/M1)^{\frac{1}{2}}$ agrees well with our previous measurements.[28] We have reinterpreted the original yield measurements[18] using the revised values for α_T which take into account the effect of the finite size of the nucleus. A comparison of the reduced transition probabilities for low-lying

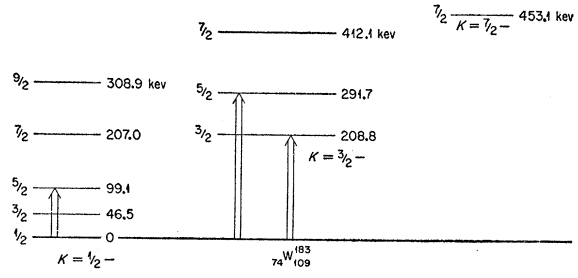

E(kev)	TRANSITION	$B(E2)_{THEORY}\times10^{48}$	$B(E2)_{EXP}\times10^{48}$	$B(M1)_d$
99.1	$1/2\longrightarrow5/2$	2.2 cm^4	2.7 cm^4	
208.8	$1/2\longrightarrow3/2$	0.099	0.049	
294.7	$1/2\longrightarrow5/2$	0.30	0.25	
84.7	$5/2\longrightarrow7/2$			0.51
82.9	$5/2\longrightarrow3/2$			0.095
192.6	$5/2\longrightarrow5/2$			0.0034
52.6	$5/2\longrightarrow3/2$			0.0066

FIG. 15. Energy level diagram of low-lying levels in W^{183} and reduced transition probabilities for several of the transitions.

[33] Cork, Brice, Nester, LeBlanc, and Martin, Phys. Rev. **89**, 1291 (1953).
[34] E. M. Bernstein and H. W. Lewis, Phys. Rev. **105**, 1524 (1957).
[35] Murray, Boehm, Marmier, and DuMond, Phys. Rev. **97**, 1007 (1955).
[36] A. W. Sunyar, Phys. Rev. **95**, 626 (1954).
[37] A. K. Kerman, Kgl. Danske Videnskab. Selskab, Mat.-fys. Medd. **30**, No. 15 (1956).

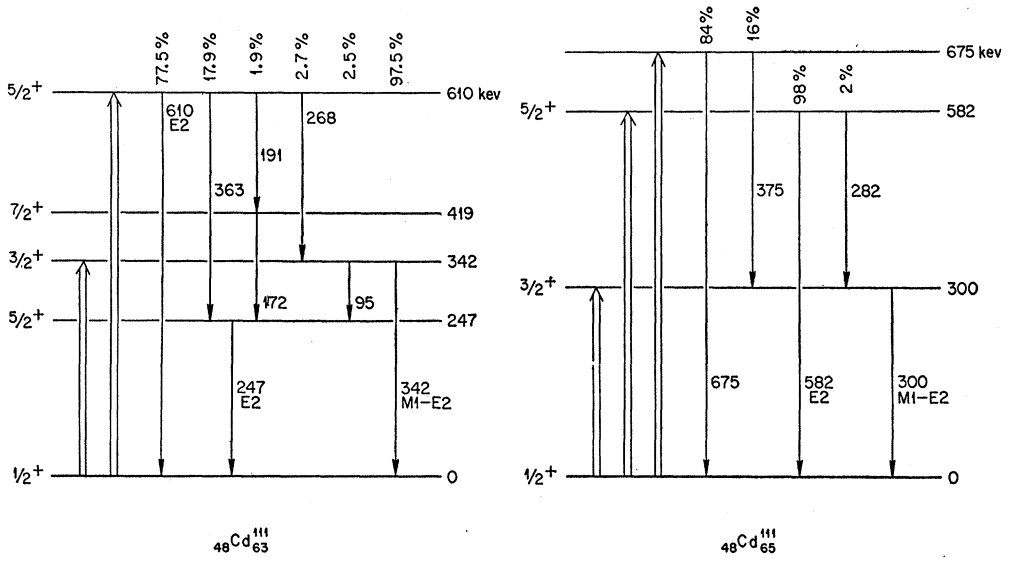

FIG. 16. Energy level diagrams of low-lying levels in Cd^{111} and Cd^{113}. The indicated decay intensities from a given level are for total transitions. *Note added in proof.*—The energy level diagram on the right should read $_{48}Cd_{65}^{113}$.

transitions in Ta^{181} with the predictions of the collective model has already been presented.[38]

G. Cadmium

Other workers[39,40] have found, by the use of targets enriched in isotopes Cd^{113} and Cd^{111}, gamma rays of 290 and 340 kev. In addition to these gamma rays we have observed gamma rays of 582 and 675 kev in Cd^{113} and of 250 and 610 kev in Cd^{111} with $E_p=2.1$ to 3.3 Mev. These gamma rays are attributed to direct excitation of levels at 300, 582, and 675 kev in Cd^{113} and at 342 and 610 kev in Cd^{111}. Furthermore, in addition to those γ rays shown in Figs. 10 and 11, coincidence spectrum measurements have revealed a number of other γ rays resulting from the decay of these levels. For Cd^{113}, gamma rays of 282 and 375 kev are observed in coincidence with the 300-kev gamma ray. For Cd^{111}, gamma rays of 95, 172, 191, and 363 kev are observed in delayed coincidence with the 250-kev gamma ray and a gamma ray of 268 kev is observed in coincidence with the 342-kev gamma ray. The intensities of these weak decay branches obtained from the coincidence spectra have been included in the analysis of our yield measurements to deduce the $B(E2)_{\text{exc}}$ given in Table VI.

The isotopic enrichments of the cadmium targets were not very large. As a result, the elimination of the contribution of the other isotopes in the targets to the angular distribution reduced the accuracy of the measurements. The angular distribution measurements of the 582- and 610-kev gamma rays in Cd^{113} and Cd^{111} are consistent with a transition assignment of $\frac{5}{2}(E2)\frac{1}{2}$. In the case of the 300- and 342-kev transitions the angular distributions were equally well fitted by two rather different values for $(E2/M1)^{\frac{1}{2}}$. A polarization direction correlation measurement clearly removed the ambiguity in the value of δ.

Energy level diagrams of low-lying levels in Cd^{111} and Cd^{113} are shown in Fig. 16. Only the low-lying states and transitions observed in Coulomb excitation are shown. The indicated intensities of the various decay branches from a given state are for transitions (gamma-ray transitions plus transitions by internal conversion).

H. Silver

Several groups of workers[9] have observed direct excitation of two levels in Ag^{109} and Ag^{107} by the use of enriched isotopes. There is reasonable agreement among the various groups on the position of these levels but there is a considerable spread ($\sim 50\%$) in the values of the $B(E2)_{\text{exc}}$. We were able to assign a spin of $\frac{5}{2}$ to the second excited state in Ag^{109} and Ag^{107} from our angular measurements[28] using targets of normal silver. The angular distribution of the gamma radiation from the first excited state in Ag^{109} and Ag^{107} could be fitted equally well by two rather different values for δ.[28]

We have made additional studies of Coulomb excitation in silver using enriched targets of Ag^{107} and Ag^{109}. In addition, measurements have been made with thick and thin targets of normal silver in order to reduce the uncertainty that existed in the rate of energy loss of protons in the target materials.[7] This source of error is reflected directly in the determination of $B(E2)_{\text{exc}}$ from thick-target yields. The angular distributions of the 309-kev gamma ray in Ag^{109} and of the 324-kev gamma ray in Ag^{107} are quite similar. A polarization-direction correlation measurement has removed the ambiguity in the value of δ. Our new results for $B(E2)_{\text{exc}}$ in Ag^{109} and Ag^{107}, which agree quite well with our

[38] P. H. Stelson and F. K. McGowan, Phys. Rev. **105**, 1346 (1957).
[39] G. M. Temmer and N. P. Heydenburg, Phys. Rev. **98**, 1308 (1955).
[40] Mark, McClelland, and Goodman, Phys. Rev. **98**, 1245 (1955).

TABLE VII. A comparison of some of the quantities measured by experiment and predicted by the theory of nuclear rotational transitions, as developed by Bohr and Mottelson.

Isotope	I	E_2/E_1		$B(E2)_1/B(E2)_2$		$B(E2)_{d_{21}}/B(E2)_{d_2}$		$B(M1)_{d_{21}}/B(M1)_{d_1}$	
		Theory	Experiment	Theory	Experiment	Theory	Experiment	Theory	Experiment
$_{73}Ta^{181}$	$\frac{7}{2}$	2.22	2.23±0.04	3.89	3.74±0.42	4.71	6.6 ±1.2	1.53	2.2±0.8
$_{75}Re^{185}$	$\frac{5}{2}$	2.29	2.24±0.05	2.86	2.80±0.40	3.03	2.4 ±0.5	1.45	...
$_{75}Re^{187}$	$\frac{5}{2}$	2.29	2.25±0.05	2.86	2.29±0.33	3.03	2.6 ±0.5	1.45	...
$_{77}Ir^{191}$	$\frac{3}{2}$	2.40	2.59±0.05	1.80	...	1.50	...	1.34	...
$_{77}Ir^{193}$	$\frac{3}{2}$	2.40	2.55±0.05	1.80	1.22±0.18	1.50	0.33±0.08	1.34	5.7±3.4

earlier results obtained from targets of normal silver, are about 25 to 50% larger than those obtained by other groups.[9] Most of the discrepancy must be in the gamma-ray yield measurements and cannot be traced to the choice of α_T because the total internal conversion coefficients are small.

I. Rh^{103}

The Coulomb excitation spectrum in Rh^{103} is quite similar to Ag^{109} and Ag^{107}, i.e., levels with $I=\frac{3}{2}$ and $\frac{5}{2}$ are directly excited.[9] The angular distribution of the 298-kev gamma radiation from the state with $I=\frac{3}{2}$ could be fitted equally well by two rather different values for δ.[28] A polarization-direction correlation measurement has removed the ambiguity.

J. Mo^{95} and Mo^{97}

Several groups of workers[9] have observed Coulomb excitation of a state at 203 kev in Mo^{95}. Of the possible spins $\frac{1}{2}$, $\frac{3}{2}$, $\frac{5}{2}$, $\frac{7}{2}$, 9/2 for the excited state only the spins $\frac{1}{2}$, $\frac{7}{2}$, and 9/2 were excluded by our angular distribution measurements. The distribution could be fitted by $\delta=0.2$ to 1.1 for $I=\frac{5}{2}$ and by $\delta=-0.5$ to -1.3 for $I=\frac{3}{2}$. A polarization-direction correlation measurement clearly excluded $I=\frac{5}{2}$ because $P(\theta=\pi/2)\leq 1.06$ for all δ and the experimental value for $P(\theta=\pi/2)$ was 1.17±0.04. Our result for $B(E2)_{\text{exc}}$ of the 203-kev state in Mo^{95} is smaller by a factor of two than that given by Temmer and Heydenburg.[41]

We observe no gamma radiation with energy less than 1.2 Mev, which can be attributed to Coulomb excitation in Mo^{97}, when targets containing 89.6% Mo^{97} are bombarded with 1.8- to 3.0-Mev protons or 9-Mev α particles.

K. Nb^{93}

We have observed gamma rays of 710- and 874-kev energy when Nb^{93} is bombarded with 2.4- to 3.0-Mev protons. The variation in gamma-ray yields appeared to follow Coulomb excitation. However, coincidence spectrum measurements indicated that both gamma rays were in coincidence with harder radiation and also in coincidence with each other. We believe this gamma radiation results from the de-excitation of Mo^{94} following proton capture in Nb^{93}. The 874-kev gamma ray is probably from the $2\rightarrow 0$ transition in Mo^{94} which is observed from Coulomb excitation studies of Mo^{94}.

L. Osmium

Since the gamma radiation from the $2\rightarrow 0$ transitions in Os^{190} and Os^{192} was used to calibrate our polarimeter, we have also made yield measurements of the gamma rays following Coulomb excitation with protons and α particles. The target was prepared by sintering the metallic powder of the normal element into a foil 150 mg/cm² thick. The $B(E2)_{\text{exc}}$ deduced from the measurements are given in Table VI. The half-life of the 155-kev state in Os^{188} is in good agreement with the direct measurement of 6.5×10^{-10} sec by Sunyar.[42] Angular distribution measurements of the 186- and 206-kev gamma rays have been reported elsewhere.[1]

V. REDUCED TRANSITION PROBABILITIES

The ratio of the excitation energies in Ta^{181}, Re^{185}, Re^{187}, and possibly Ir^{191} and Ir^{193} tends to identify these states as rotational excited states of the ground state configuration. It is therefore of interest to see how well the observed reduced transition probabilities agree with the theory of nuclear rotational transitions, as developed by Bohr and Mottelson.[5] Since the absolute transition probabilities contain an unknown intrinsic nuclear moment, only the ratio of transition probabilities predicted by the theory can be compared with experiment. A summary of the available data which provides a direct test of these intensity rules is given in Table VII. The ratio $B(E2)_1/B(E2)_2$ denotes the ratio of reduced transition probabilities for excitation to the first and second excited states and the other subscripts were defined under the section on rhenium. The agreement between theory and experiment is reasonably good for Ta^{181}, Re^{185}, and Re^{187}. The deviations in Ir^{191} and Ir^{193} are probably an indication that the excitation spectrum is not a pure rotational spectrum.

From the measured $B(M1)_d$ and the ground state magnetic moment one can calculate g_Ω, the gyromagnetic ratio of the particle configuration, and g_R, the gyromagnetic ratio of the collective motion. This information alone leads to two sets of values for g_Ω and g_R because only the absolute value of $g_\Omega-g_R$ is given

[41] G. M. Temmer and N. P. Heydenburg, Phys. Rev. **104**, 967 (1956).

[42] A. W. Sunyar, Phys. Rev. **98**, 653 (1955).

TABLE VIII. Values of g_Ω and g_R obtained from the ground-state magnetic moment, the $B(M1)_d$, and the sign of Q_0 and $(E2/M1)^{\frac{1}{2}}$. The quantity $(g_\Omega)_{\text{Nilsson}}$ was calculated using the single-particle eigenfunctions for deformed nuclei as given by Nilsson.

Nucleus	μ	Transition (kev)	$g_\Omega - g_R$	g_Ω	g_R	η	$(g_\Omega)_{\text{Nilsson}}$
Ta^{181}	2.1	136	0.407	0.69	0.29	4.3	0.41
		166	0.492	0.71	0.22		
Re^{185}	3.17	159	1.201	1.61	0.41	3.7	1.88
Re^{187}	3.20	167	1.279	1.65	0.37	3.5	1.88
Ir^{193}	0.17	140	−0.291	−0.003	0.288	2.3	−0.28
		217	−0.597	−0.126	0.471		
Au^{197}	0.14	277	−0.707	−0.190	0.517	1.3	−0.20

by $B(M1)$. However, the relative sign of the $M1$ and $E2$ transition amplitudes is determined from the angular distribution measurements. This phase is related to the sign of Q_0, the intrinsic quadrupole moment, and of $g_\Omega - g_R$ and is given by[5]

$$\text{sign}\delta = \text{sign}\left(\frac{Q_0}{g_\Omega - g_R}\right).$$

For the nuclei listed in Table VIII the spectroscopic quadrupole moment is known to be positive. Thus, the sign of $g_\Omega - g_R$ is the sign of δ given in Table VI. The values for g_Ω and g_R deduced from the experimental data are given in Table VIII. For comparison the values g_Ω, which were calculated using the single-particle eigenfunctions for deformed nuclei as given by Nilsson,[43] are also listed. The value of the deformation parameter η was chosen to fit the observed $B(E2)$ for each of these nuclei. However, the calculated value of g_Ω is insensitive to the exact value of η for these nuclei.

For even-even nuclei of the medium-weight elements, the low-lying excited states are found to exhibit a pattern which resembles that of quadrupole vibrations about a spherical equilibrium shape.[44] An alternative description in terms of the "shape unstable" model has been given by Wilets and Jean.[45] It is not clear which model describes the regularities in these even-even nuclei in a more consistent fashion. The reduced transition probabilities for excitation of the first 2+ state from Coulomb excitation experiments clearly display the collective character of these transitions.

From the $B(E2)$ and E_{2+} one can obtain the parameters B_2 and C_2 which are appropriate to a description of quadrupole vibrations about a spherical equilibrium shape for the nucleus.[46] B_2 is associated with the mass transported by the collective vibration and C_2 represents an effective surface tension. Alternatively one can obtain from the observed $B(E2)$ the deformation parameter β which is appropriate to a description in terms of the "shape unstable" model. A summary of the β determined empirically from the $B(E2)$ for even-even nuclei of medium weight has already been given.[7,41] For the heavier isotopes of Ru and Pd the values of β are comparable to those deduced from the even-even isotopes of Hf and W which do exhibit a rotational excitation spectrum. Nevertheless the excitation spectrum in the even-even isotopes of Ru and Pd is clearly not a rotational spectrum. If the "shape unstable" model is a better description for the excitation spectrum in these even-even nuclei, then one might expect that an odd nucleon coupled to a γ-unstable core would tend to stabilize the core about axial symmetry.[45] This can be tested by examining the information obtained from Coulomb excitation of odd-A nuclei.

A vibrational interpretation of the excitation spectrum of odd-A nuclei of medium weight is less well understood. One must consider, in addition to the collective motion, the coupling of the intrinsic nucleonic motion of the odd particle to the collective oscillation since the latter involves variations in the nuclear field. The effect of the coupling to the quadrupole vibration depends essentially on the parameter[9]

$$q = \left(\frac{5}{16\pi}\right)^{\frac{1}{2}} \frac{k}{(\hbar\omega_2 C_2)^{\frac{1}{2}}},$$

where k is of the order of magnitude of the average potential energy of a nucleon. For $q \sim 1$ (intermediate coupling) the treatment cannot be handled in a straightforward manner. However, for q somewhat larger than one, the last odd nucleon may appreciably polarize the nuclear core to a nonspherical equilibrium shape. In addition Alder *et al.*[9] have given an approximate sum rule for the case of intermediate coupling which states hat the $\sum B(E2)_{\text{exc}}$ for an odd-A nucleus should be approximately equal to the $B(E2, 0 \rightarrow 2)$ for a neighboring even-even nucleus. A sum greatly exceeding this value implies an appreciable polarization produced by the last nucleon and may indicate that the coupling scheme is approaching that of a deformed nucleus. Taking $k = 40$ Mev, we find q to be between 4 and 6 from the neighboring even-even nuclei about Ag^{109}, Ag^{107}, and Rh^{103}. The sum of the $B(E2)_{\text{exc}}$ is (5 to 6) $\times 10^{-49}$ cm^4 while the $B(E2, 0 \rightarrow 2)$ for the neighboring even-even nuclei are (5 to 9)$\times 10^{-49}$ cm^4. The results would imply that the coupling scheme is not approach-

[43] S. G. Nilsson, Kgl. Danske Videnskab. Selskab, Mat.-fys. Medd. **29**, No. 16 (1955).
[44] G. Scharff-Goldhaber and J. Weneser, Phys. Rev. **98**, 212 (1955).
[45] L. Wilets and M. Jean, Phys. Rev. **102**, 788 (1956).
[46] See, for instance, reference 9 where a summary of these vibrational parameters is given.

ing that of a deformed nucleus. In addition, if these nuclei are γ unstable, the odd nucleon is not tending to stabilize the core about axial symmetry.

Nilsson has also given a relation,[43]

$$3\mu=(g_l-g_R)a-\tfrac{1}{2}g_s+g_l+g_R,$$

between the magnetic moment and the decoupling factor a, which appears in the expression for rotational energy for odd-A nuclei with $\Omega=\frac{1}{2}$. This relation is applicable for $I_0=\Omega=K=\frac{1}{2}$ and odd parity. Using free nucleon values for g_l and g_s and taking $a\approx\frac{2}{3}$, which is deduced from the observed levels in Ag^{109}, Ag^{107}, and Rh^{103}, we find $g_R\approx 2$. This result would imply that the excitation spectrum in Ag^{109}, Ag^{107}, and Rh^{103} is not rotational.

From the even-even nuclei of cadmium q is 2.5 and the sum of the $B(E2)_{\text{exc}}$ in Cd^{113} and Cd^{111} is 5.0 and 2.5×10^{-49} cm^4, respectively, while the $B(E2,\ 0\rightarrow 2)$ for Cd^{114}, Cd^{112}, and Cd^{110} are between 5.0 and 5.8×10^{-49} cm^4. In the region of Mo^{95} and Mo^{97} q is 1.8 and the sum of the $B(E2)_{\text{exc}}$ is 0.35×10^{-49} cm^4 for Mo^{95} while the $B(E2,\ 0\rightarrow 2)$ for Mo^{94} and Mo^{96} are 2.7 and 3.0×10^{-49} cm^4. Alder *et al.*[9] have pointed out that, when the $\sum B(E2)_{\text{exc}}$ in odd-A nuclei is appreciably smaller than the $B(E2,\ 0\rightarrow 2)$, one may conclude that there exist strong quadrupole transitions as yet undetected. In the case of Mo^{95}, Mo^{97}, or Nb^{93}, it seems rather unlikely that we may have missed detecting any strong quadrupole transitions with an excitation energy less than 1 Mev.

VI. CONCLUSIONS

From the angular distribution measurements, the spins of twenty excited states in odd-mass nuclei have been assigned. The gamma radiation from the de-excitation of fifteen of these states was mixed $M1$-$E2$ radiation and the ratio $(E2/M1)^{\frac{1}{2}}$ was determined from the angular distributions. Measurements of the polarization-direction of the radiation from 9 transitions have resolved the ambiguity either in the value of $(E2/M1)^{\frac{1}{2}}$ or in the spin of the excited state. In the case of transitions in Tl^{205}, Tl^{203}, and Mo^{95}, a polarization-direction measurement provided a more accurate measurement of $(E2/M1)^{\frac{1}{2}}$. This information combined with the cross section for excitation has yielded the $B(M1)_d$ for 16 transitions.

In the past, polarization-direction correlation measurements of successive nuclear transitions were performed primarily to determine the relative parities of excited states involving the emission of pure multipole radiation. In this case, if the angular distribution were isotropic, the polarization-direction correlation was also isotropic, i.e., $P(\theta)=1$. For mixed transitions, if the angular distribution is isotropic, the polarization-direction correlation is not necessarily isotropic, i.e., $P(\theta)\neq 1$. As an example, the directional correlation for the sequence $\frac{1}{2}(Q)\frac{3}{2}(E2+M1)\frac{1}{2}$ is isotropic for $(E2/M1)^{\frac{1}{2}}=-3.65$ but $P(\theta=\pi/2)$ is 2.52 if the polarization-direction of the mixed radiation is measured. Such a case has already been encountered in our measurements. The angular distribution of the 300-kev gamma ray following Coulomb excitation in Cd^{113} was nearly isotropic but the polarization-direction correlation was quite large.

Information obtained from Coulomb excitation of odd-mass nuclei does not appear to enable one to decide whether the "free vibration" or the "shape unstable" model gives a better description of the regularities observed in the neighboring even-even nuclei.